Journal of Power Sources 265 (2014) 201–213

Contents lists available at ScienceDirect

Journal of Power Sources

journal homepage: www.elsevier.com/locate/jpowsour

Experimental advances and preliminary mathematical modeling of the Swiss-roll mixed-reactant direct borohydride fuel cell

Amin Aziznia, Colin W. Oloman, Előd L. Gyenge*

Department of Chemical and Biological Engineering, Clean Energy Research Center, The University of British Columbia, 2360 East Mall, Vancouver, BC V6T 1Z3, Canada

HIGHLIGHTS

- Engineering advancements presented for the Swiss-roll mixed reactant borohydride–oxygen alkaline fuel cell.
- High power density (2500 W m^{-2}) and excellent durability demonstrated with Pt–Ag anode–cathode catalyst combination.
- The role of porous diaphragm separator and fluid distributor metallic mesh pore size is demonstrated.
- First preliminary mathematical model of the mixed reactant borohydride–oxygen fuel cell.

GRAPHICAL ABSTRACT

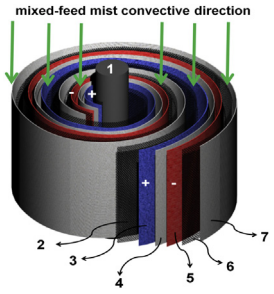

ARTICLE INFO

Article history:
Received 21 October 2013
Received in revised form
19 March 2014
Accepted 10 April 2014
Available online 4 May 2014

Keywords:
Swiss-roll mixed-reactant fuel cell
Direct borohydride fuel cell
Alkaline fuel cell
MnO_2 oxygen reduction catalyst
Mixed-potential

ABSTRACT

The Swiss-roll single-cell mixed reactant (SR-MRFC) borohydride – oxygen fuel cell equipped with Pt/carbon cloth 3D anode and either MnO_2 or Ag gas-diffusion cathodes is investigated by a combination of experimental studies and preliminary mathematical modeling of the polarization curve. We investigate the effects of four variables: cathode side metallic mesh fluid distributor, separator type (Nafion 112® vs. Viledon®), cathode catalyst (MnO_2 vs. Ag), and the hydrophilic pore volume fraction of the gas-diffusion cathode. Using a two-phase feed of alkaline borohydride solution (1 M $NaBH_4$ – 2 M NaOH) and O_2 gas in an SR-MRFC equipped with Pt/C 3D anode, MnO_2 gas diffusion cathode, Viledon® porous diaphragm, expanded mesh cathode-side fluid distributor, the maximum superficial power density is 2230 W m^{-2} at 323 K and 105 kPa(abs). The latter superficial power density is almost 3.5 times higher than our previously reported superficial power density for the same catalyst combinations. Furthermore, with a Pt anode and Ag cathode catalyst combination, a superficial power density of 2500 W m^{-2} is achieved with superior performance durability compared to the MnO_2 cathode. The fuel cell results are substantiated by impedance spectroscopy analysis and preliminary mathematical model predictions based on mixed potential theory.

1. Introduction

The conventional design of proton exchange membrane (PEM) fuel cell stacks is based on a plate-and-frame in series architecture that evolved from Volta's original concept of the zinc-air battery stack. The performance, durability and cost of the various

* Corresponding author.
E-mail address: egyenge@chbe.ubc.ca (E.L. Gyenge).

http://dx.doi.org/10.1016/j.jpowsour.2014.04.037
0378-7753/

Nomenclature

a	electrode specific surface area ($m^2\ m^{-3}$)
$C_{BH_4^-}^{inlet}$	inlet concentration of sodium borohydride (mol m^{-3})
$C_{O_2}^{air}$	inlet concentration of oxygen in air (mol m^{-3})
$C_{O_2}^{inlet}$	inlet concentration of oxygen in O_2 (mol m^{-3})
C_{NaOH}^{inlet}	inlet concentration of NaOH (mol m^{-3})
C_i	concentration of component i (mol m^{-3})
$D_{BH_4^-}$	BH_4^- diffusion coefficient ($m^2\ s^{-1}$)
$D_{BH_4^-}^{eff}$	effective BH_4^- diffusion coefficient ($m^2\ s^{-1}$)
$E^{\circ}_{BOR\ 298\ K}$	standard potential of BOR at 298 K (V_{SHE})
$E^{\circ}_{ORR\ 298\ K}$	standard potential of BOR at 298 K (V_{SHE})
E_a	anode potential (V_{SHE})
E_a^{OCP}	anode open circuit potential ($V_{MMO\ or\ SHE}$)
E_a^e	equilibrium potential of BOR (V_{SHE})
E_c	cathode potential (V_{SHE})
E_c^{OCP}	cathode open circuit potential ($V_{MMO\ or\ SHE}$)
E_c^e	equilibrium potential of ORR (V_{SHE})
$E_{cell\ (j)}$	cell voltage at current density of j (V)
K_a	local mass transfer coefficient of anode (m s^{-1})
K_c	global cathode mass transfer coefficient (m s^{-1})
$K_{m,i}$	mass transfer coefficient of component i (m s^{-1})
P_{O_2}	partial pressure of oxygen in feed (kPa(abs))
$R_{contact}$	electronic plus contact resistance (Ohm m^2)
d_{cloth}	carbon cloth fiber diameter (m)
$j_{BOR_{MnO_2}}$	current density of BOR on MnO_2 ($A\ m^{-2}$)
$j_{BOR_{Pt}}$	current density of BOR on Pt ($A\ m^{-2}$)
$j_{L_{O_2}}^a$	limiting current density of ORR in anode ($A\ m^{-2}$)
$j_{L_{air}}$	limiting current density of cathode in air ($A\ m^{-2}$)
$j_{ORR_{MnO_2}}$	current density of ORR on MnO_2 ($A\ m^{-2}$)
$j_{ORR_{Pt}}$	current density of ORR on Pt ($A\ m^{-2}$)
$j_{o,BOR_{MnO_2}}$	apparent exchange current density of BOR on MnO_2 ($A\ m^{-2}$)
$j_{o,BOR_{Pt}}$	apparent exchange current density of BOR on Pt ($A\ m^{-2}$)
$j_{o,ORR_{MnO_2}}$	apparent exchange current density of ORR on MnO_2 ($A\ m^{-2}$)
$j_{o,ORR_{Pt}}$	apparent exchange current density of ORR on Pt ($A\ m^{-2}$)
$j_{L,i}$	limiting current density of component i ($A\ m^{-2}$)
$j_{L,i}$	limiting current density of component i ($A\ m^{-2}$)
j_{L,BH_4}	local limiting current density of BH_4^- ($A\ m^{-2}$)
j_L^a	effective BH_4^- mass transfer limiting current density in 3D anode ($A\ m^{-2}$)
j_L^c	limiting current density of O_2 cathode ($A\ m^{-2}$)
j_e	ionic current density ($A\ m^{-2}$)
j_{net}	net current density ($A\ m^{-2}$)
j_s	electronic current density ($A\ m^{-2}$)
n_{BOR}	number of electron transferred in BOR reaction (8)
n_{ORR}	number of electron transferred in ORR reaction (4)
n_{rds}^a	number of electron transferred in rate determining step of BOR
n_{rds}^c	number of electron transferred in rate determining step of ORR
t'	electro-active thickness of 3D electrode (m)
F	Faradic constant (96,485 C mol^{-1})
P	oxidant pressure (kPa(abs))
R	Universal gas constant (8.314 J $mol^{-1}\ K^{-1}$)
T	temperature (K)
j	current density ($A\ m^{-2}$)
t	time (s)

Symbols containing Greek letters

ΔV	potential drop in the anolyte under mass transfer control
ΔS_{BOR}	standard entropy change of BOR (J K^{-1} mol^{-1})
ΔS_{ORR}	standard entropy change of ORR (J K^{-1} mol^{-1})
$\Delta\phi_{R_{contact}}$	contact resistance voltage drop (V)
$\Delta\phi_{ACL}^{ionic}$	ionic Ohmic voltage drop across ACL (V)
$\Delta\phi_{GDE}^{ionic}$	ionic Ohmic voltage drop across GDE (V)
$\Delta\phi_{Ohm}$	total Ohmic voltage drop (V)
$\Delta\phi_{sep}$	Ohmic drop over separator (V)
$\alpha_{BOR}^{MnO_2}$	charge transfer coefficient of BOR on MnO_2
α_{BOR}^{Pt}	charge transfer coefficient of BOR on Pt
$\alpha_{ORR}^{MnO_2}$	charge transfer coefficient of ORR MnO_2
α_{ORR}^{Pt}	charge transfer coefficient of ORR on Pt
δ_{ACL}	carbon cloth thickness (m)
δ_{GDE}	gas diffusion electrode thickness (m)
δ_{sep}	separator thickness (m)
ε_{ACL}	ACL (carbon cloth) porosity
ε_{GDE}	GDE porosity
ε_d	diaphragm porosity
$\kappa_e^{298\ K}$	effective ionic conductivity of electrolyte at 298 K (mho m^{-1})
$\kappa_e^{323\ K}$	effective ionic conductivity of electrolyte at 323 K (mho m^{-1})
κ_e^T	effective ionic conductivity of electrolyte at temperature T (mho m^{-1})
κ_{eff}	effective electrolyte conductivity (mho m^{-1})
κ_{eff}^{ACL}	effective electrolyte conductivity in ACL
κ_{eff}^{GDE}	effective ionic conductivity of GDE (mho m^{-1})
κ_{eff}^{sep}	effective ionic conductivity of separator (mho m^{-1})
λ	volume fraction of liquid in ε_{ACL}
ν	scan rate (V s^{-1})
τ	hydrophilic pore fraction of ε_{GDE}
ω	liquid volumetric flow rate ($m^3\ s^{-1}$)

Abbreviations

3D	3-dimensional
ACL	anode catalyst layer
BOR	borohydride oxidation reaction
CE	counter electrode
CV	cyclic voltammetry
DBFC	direct borohydride fuel cell
EIS	electrochemical impedance spectroscopy
GDE	gas diffusion electrode
MMO	mercury/mercury oxide
MRFC	mixed-reactant fuel cell
OCP	open circuit potential
OCV	open circuit voltage
ORR	oxygen reduction reaction
PEM	proton/polymer exchange membrane
RE	reference electrode
RHE	reversible hydrogen electrode
SEM	scanning electron microscopy
SHE	standard hydrogen electrode
SR-MRFC	Swiss-roll mixed-reactant fuel cell
SS	stainless steel
WE	working electrode